

NUMERICAL STUDY OF YANG-MILLS CLASSICAL SOLUTIONS ON THE TWISTED TORUS

M. García Pérez* and A. González-Arroyo†

*Departamento de Física Teórica C-XI
Universidad Autónoma de Madrid
28049 Madrid, Spain*

We use the lattice cooling method to investigate the structure of some gauge fixed $SU(2)$ Yang-Mills classical solutions of the euclidean equations of motion which are defined in the 3-torus with symmetric twisted boundary conditions.

*Bitnet address: MARGA@EMDUAM11

†Bitnet address: ARROYO@EMDUAM11

1 Introduction

In this paper we will analyse an $SU(2)$ Yang-Mills field configuration which is periodic in 3-space and tends to a pure gauge in both $t = \pm\infty$. This configuration is a solution of the classical euclidean equations of motion and has infinite action and topological charge (finite within one unit cell). The configuration arises naturally when one studies gauge fields on the spatial torus with twisted boundary conditions (t.b.c.) [1]. In particular, we fix the torus to have equal period in all three directions and a twist vector $\vec{m} = (1, 1, 1)$. The presence of the torus breaks down the $SO(3)$ rotational symmetry down to the cubic group. If we fix, without loss of generality, the length of the spatial torus to $l = 1$, we may write the boundary conditions

$$\mathbf{A}_\mu(x + \hat{e}_i) = \sigma_i \mathbf{A}_\mu(x) \sigma_i \quad (1.1)$$

where σ_i are the Pauli matrices and \hat{e}_i the unit vector in the i^{th} direction. The choice of the Pauli matrices as the twist matrices can be regarded as a partial gauge fixing of the problem. The remaining group of gauge transformations must satisfy

$$\mathbf{\Omega}(x + \hat{e}_i) = \sigma_i \mathbf{\Omega}(x) \sigma_i \quad (1.2)$$

This is not, however, the most general internal symmetry transformation of our problem. One can perform a transformation

$$\mathbf{A}_\mu(x) \rightarrow \mathbf{A}'_\mu(x) = \mathbf{\Omega}^{(z)}(x) \mathbf{A}_\mu(x) \mathbf{\Omega}^{(z)\dagger}(x) + i \mathbf{\Omega}^{(z)}(x) \partial_\mu \mathbf{\Omega}^{(z)\dagger}(x) \quad (1.3)$$

with

$$\mathbf{\Omega}^{(z)}(x + \hat{e}_i) = z_i \sigma_i \mathbf{\Omega}^{(z)}(x) \sigma_i \quad (1.4)$$

and $z_i = \pm 1$. This transformation preserves the b.c. Eq.(1.1) and leaves the Yang-Mills action invariant. Nevertheless, if $z_i \neq 1$ for some $i = 1, 2, 3$ the transformation is not, strictly speaking, a gauge transformation since it modifies the values of the Wilson loops associated with non-contractible loops (Polyakov loops):

$$W(\gamma) \rightarrow W'(\gamma) = z_i^{\omega_i(\gamma)} W(\gamma) \quad (1.5)$$

where $\omega_i(\gamma)$ is the winding number of the loop in the i^{th} direction. We will call these transformations singular gauge transformations and the group of these transformations (modulo ordinary gauge transformations) is isomorphic to Z_2^3 . As we will see later, these transformations act non-trivially on our gauge field configuration and thus we have 8 configurations rather than one.

The configuration with smallest action ($S=0$) with our boundary conditions is of the pure gauge form:

$$\mathbf{A}_\mu(x) = i \mathbf{\Omega}^{(z)}(x) \partial_\mu \mathbf{\Omega}^{(z)\dagger}(x) \quad (1.6)$$

with $\mathbf{\Omega}^{(z)}(x)$ satisfying Eq.(1.4). However, it turns out [2] that there are only two gauge non equivalent configurations of this type, those with $z_i = 1$ for all i , and $z_i = -1$ for all i . In the $\mathbf{A}_0 = 0$ gauge these configurations are constant in time and equal to the minima of the potential energy $\sum_i Tr B_i^2$. The problem becomes that of a Z_2 symmetric

potential with two non-symmetric minima. The order parameter distinguishing these two is the Polyakov loop winding the torus once along each direction ($\omega_i = 1$). Just as in the case of the $\lambda\phi^4$ potential (and negative mass squared), we can investigate the solution which interpolates between the two minima as time goes from $-\infty$ to $+\infty$. This is an instanton solution and gives rise to the leading weak coupling contribution to the energy splitting between the Z_2 symmetric and antisymmetric states.

These instanton configurations are precisely the solutions which we are after. They have half integer topological charge and are precisely the minimum action configurations in a 4-torus with infinite length and with t.b.c. both in time and space. The twist in time $n_{0i} = 1$ eliminates the constant minima solutions.

The existence of these configurations was proved by Sedlacek [3]. In a previous paper [4] we investigated the behaviour of these solutions by using the lattice approximation and the cooling method [5]. There it was shown that the total action and energy of the lattice minimum action configurations scale towards a continuum value. The value of the continuum action is very close to $4\pi^2$, the absolute minimum for a topological charge Q of $1/2$. Indeed, this minimum is only attained by a self-dual or anti-self-dual configuration, so our configurations must be very approximately, if not exactly, self-dual. If we perform a parity transformation to this self-dual instanton configuration we get an anti-self-dual anti-instanton configuration with $Q = -1/2$.

The purpose of this paper is to report a more extensive and accurate analysis of the lattice minimum configurations in order to answer some questions which were not settled by our previous paper. Apart from giving additional support to the question of scaling towards the continuum and self-duality, we have shown that there are indeed eight different gauge-inequivalent configurations (four instantons and four anti-instantons) which can be obtained by acting with the group of singular gauge transformations on one of them. All these configurations are non abelian and cubic-symmetric. We have obtained functional expressions for the various physical quantities, including the vector potentials and field strengths in a suitable gauge, which describe their qualitative features. Satisfactory quantitative description of the data has been obtained by using these functional expressions and the first few terms in a Fourier expansion of the functions involved. We also report the steps that we have taken in the direction of finding an analytic expression for the solution. Although our attempts in this respect have not achieved the ultimate goal, we have explored several paths involving some lengthy and non-trivial manipulations, and our results can be of great help for future investigations.

Our solution, being non-abelian, is very different to the abelian solutions [6] which are known to exist for other twists, other values of the topological charge and additional periodicity in time. However, it is much more similar to the instanton solution on $S_3 \times \mathfrak{R}$. In a recent paper [7] this solution has been used to investigate the θ -dependence beyond the steepest descent. It is in this spirit that our solution is physically relevant. The reader is addressed to Ref.7 and the earlier Ref.8 to see the role of our instanton solution for the Yang-Mills dynamics, in the weak coupling limit.

2 Analysis of the data

Our strategy has been explained in Ref.4. We consider an $N_s^3 \times N_t$ lattice with twisted boundary conditions. We use cooling to obtain configurations with smaller and smaller action. We stop once the value of the action has changed by less than 10^{-4} over the last 100 cooling sweeps. To perform the analysis reported here we have used the configurations which we employed in Ref.4 together with new data which extend over larger lattices $(N_s, N_t) = (11, 29)$ and $(15, 29)$. We have little to add to the results of Ref.4 concerning integrated quantities. The new data just give extra support to the conclusions presented there. The value of the action S is 39.234 and 39.347, for $(11, 29)$ and $(15, 29)$ in agreement with our extrapolation formula $S = 4\pi^2 - 29.7a^2$ (with $a = 1/N_s$). The degree of self duality is now $X = 2\frac{|S_E - S_B|}{S_E + S_B} = 0.0045$ and 0.0033 for the same two lattices. We notice that the errors introduced by the lattice approximation are smaller than 1% for integral quantities. This can be explained by the fact that they are $O(a^2)$. In the case of the vector potentials and the colour electric and magnetic fields at a given point $A_i^a(x)$, $E_i^a(x)$ and $B_i^a(x)$, we expect errors of order a : typically then 10% for our values of N_s . One can estimate more precisely the size of these errors by several methods. For example comparing E_i^a and B_i^a at the same point the difference is never greater than 0.14 (representing 3% of the magnitude at those points). On the average a difference of order 0.04 makes the χ^2 per degree of freedom of the comparison of order 1. Other estimates of the errors can be deduced by comparing values for different N_s or by using different lattice approximants to the continuum value. The resulting errors depend on the quantity under consideration and on the value of t , but stay within a factor of two of 0.04 in all cases. We have chosen, thus, the value of 0.04 as a typical error which we will be using in all χ^2 fits of the data.

2.1 Gauge invariant quantities

We start analysing the structure of our solution by looking at gauge invariant quantities. Consider first the colour electric and magnetic fields E_i^a , B_i^a . They can be regarded as six vectors in the 3-dimensional colour space. Gauge transformations amount to rotations in this space. Thus, the gauge invariant quantities are the scalar products and moduli of these vectors $M_{ij} = \vec{E}_i \cdot \vec{E}_j$. Due to the approximate self-duality the colour magnetic fields give the same information within errors. Before stating the results of our analysis let us mention one technical point. Our interest is centered on the values of these quantities in the continuum limit. To extract these values one can use various lattice quantities all of which differ by an amount of order a . Nevertheless, in checking certain symmetries, it is essential to choose lattice observables which respect the lattice symmetry. For that reason we have extracted the colour field strength at each lattice point, $F_{\mu\nu}^b(na)$, by averaging the four plaquettes attached to that point in each $\mu\nu$ plane:

$$F_{\mu\nu}^b(na) = \frac{1}{4a^2} Tr \{ -i\sigma_b [\mathbf{P}_{\mu\nu}(n) + \mathbf{P}_{\nu-\mu}(n) + \mathbf{P}_{-\nu\mu}(n) + \mathbf{P}_{-\mu-\nu}(n)] \} \quad (2.1)$$

where, for instance, $\mathbf{P}_{\nu-\mu}(n)$ stands for the following product of lattice links: $\mathbf{P}_{\nu-\mu}(n) = \mathbf{U}_\nu(n) \mathbf{U}_\mu^\dagger(n - \hat{\mu} + \hat{\nu}) \mathbf{U}_\nu^\dagger(n - \hat{\mu}) \mathbf{U}_\mu(n - \hat{\mu})$. The previous quantity transforms in the right way under gauge transformations and is symmetric under cubic transformations around the point na .

The main features of the solution are the following:

- a) At each time value there is a point of maximum energy density, which we will call the spatial center of the instanton, whose coordinates are time-independent and we will choose them as $\vec{x} = \vec{0}$. Furthermore there is a time where the energy is maximal and we will choose it as the origin of time, $t = 0$. Our solution is cubic invariant with respect to the spatial center and invariant under time reversal. The spatial center is not one of the lattice points, but it can be located by interpolation. The same is true for the origin of time.
- b) For all times and at the spatial center of the instanton one has $M_{ij} \propto \delta_{ij}$. This orthogonality implies that the solution is not abelian. Away from the center the vectors E_i^a cease to be mutually orthogonal but they are never collinear.
- c) We have fitted the moduli and scalar products at $t = 0$ to the first terms in a Fourier expansion. Our results are

$$\begin{aligned}
M_{11} = & \cos^2(\pi x) \{ 15.00 + 20.02 [\phi(y) + \phi(z)] \\
& -3.12 \cos^2(\pi y)\cos^2(\pi z) + 0.128 \sin^2(2\pi y)\sin^2(2\pi z) \\
& -0.18 [\cos^2(\pi y)\sin^2(2\pi z) + \cos^2(\pi z)\sin^2(2\pi y)] \} \\
& +32.74 \phi(y)\phi(z) \\
& -\sin^2(2\pi x) \{ 0.232 + 2.25 [\cos^2(\pi y) + \cos^2(\pi z)] \\
& +0.80 \cos^2(\pi y)\cos^2(\pi z) \}
\end{aligned} \tag{2.2}$$

$$M_{12} = -1.608 [1 - 0.433 \cos(2\pi z)] \chi(x) \chi(y) \tag{2.3}$$

where

$$\begin{aligned}
\phi(x) &= \cos^2(\pi x) - 0.082 \sin^2(2\pi x) \\
\chi(x) &= \sin(2\pi x) + 0.086 \sin(4\pi x)
\end{aligned}$$

The quality of the fit is very good (see fig.1 for example). The remaining components are just obtained by the appropriate replacement of the indices and variables in the previous expression, in a way which is consistent with cubic invariance and parity invariance. Notice that \vec{E}_i^2 vanishes when $x_i = \pm 1/2$ and $x_j = \pm 1/2$. Notice also that the solution seems perfectly smooth.

We turn now our attention to non local gauge invariant quantities: the Polyakov loops. Due to the boundary conditions these variables are defined as

$$\Omega_\mu(x) = \text{Tr} \left\{ \exp \left[i \int_{\gamma_\mu(x, x')} \mathbf{A}_\nu dx^\nu \right] \Gamma_\mu(x') \exp \left[i \int_{\gamma_\mu(x', x)} \mathbf{A}_\nu dx^\nu \right] \right\} \tag{2.4}$$

where $\gamma_\mu(a, b)$ is a straight line in the positive μ direction starting at a and ending at b , x' is the border of the torus patch, Tr is the ordered exponential and $\Gamma_\mu(x)$ the twist matrices. On the lattice these quantities are simply given by the ordered product of the

μ -links corresponding to the path $\gamma_\mu(x)$. These quantities transform like \mathbf{E}_i under gauge transformations and therefore the gauge invariant quantities are just the scalar products in colour space $\frac{1}{2}Tr(\mathbf{\Omega}_\mu(x)\mathbf{\Omega}_\nu(x)) = X_{\mu\nu}(x)$ and the traces themselves $\frac{1}{2}Tr(\mathbf{\Omega}_\mu(x)) = X_\mu(x)$.

Since our instanton evolves in time from one pure gauge Eq.(1.6) ($z_i = 1$) to another gauge inequivalent one ($z_i = -1$), and a representative of each class is given by $\mathbf{\Omega}_i(x) = \pm i\sigma_i$ ($i = 1, 2, 3$), we expect $X_{ij} = -\delta_{ij}$, $X_i = 0$ for large $|t|$. Indeed our results agree with this situation. As a matter of fact X_μ can be fitted with a $\chi^2 = 0.005$ per degree of freedom (with an absolute error of 0.04) to the formula

$$X_\mu = \prod_{\nu \neq \mu} m_\nu \quad (2.5)$$

where $m_i = m(x_i)$ for $i = 1, 2, 3$ and $m_0 = m_0(t)$. This is a very remarkable factorization property. The function m is parametrised as

$$m(x) = \cos(\pi x)(1 + C \sin^2(\pi x)) \quad (2.6)$$

where $C = -0.196$ and $m_0(t)$ is given in Fig.2. Notice as well that the m functions are antiperiodic. Thus, by translating our solution by one period in any direction we get a new solution. In this fashion one generates 4 solutions out of one. Thus, we are not dealing with a unique instanton solution but rather with a family of solutions related by singular gauge transformations.

2.2 Gauge dependent quantities

In order to extract all the information from our numerical results we have to obtain also gauge dependent information. In particular, one would like to extract the gauge potentials themselves in a suitable gauge. This turns out to be feasible and our results are presented in what follows.

First of all one must introduce a simple gauge fixing, which respects most of the symmetry of the problem. It is natural to select $\mathbf{A}_0 = 0$, a condition which preserves all spatial symmetries. To completely specify the gauge one has to fix the remaining time-independent gauge transformations. This can be done by fixing $\vec{A}(\vec{x}, t = -\infty) = \vec{0}$ or equivalently $\mathbf{\Omega}_i(\vec{x}, t = -\infty) = i\sigma_i$. This fixes the gauge completely including global gauge rotations. At $t = +\infty$ the gauge fields must coincide with a pure gauge Eq.(1.6) and in the $A_0 = 0$ gauge this gauge transformation is indeed given by the temporal Polyakov loop $\mathbf{\Omega}_0(\vec{x}, t = -\infty)$. Notice that $\mathbf{\Omega}_0$ transforms precisely like Eq.(1.4) for $z_i = -1$. The exact form of $\mathbf{\Omega}_0(\vec{x}, t = -\infty)$ can be obtained in terms of the gauge invariant quantities $\frac{1}{2}Tr(\mathbf{\Omega}_0(\vec{x}, t = -\infty))$ and $\frac{1}{2}Tr(\mathbf{\Omega}_0(\vec{x}, t = -\infty) \cdot \mathbf{\Omega}_i(\vec{x}, t = -\infty))$. These have been obtained from our data and the result can be summarised by giving a functional form which describes these data with a $\chi^2 = 0.01$ per degree of freedom

$$\mathbf{\Omega}_0(\vec{x}, t = -\infty) = m(x)m(y)m(z) I + i \sqrt{1 - \prod_i m_i^2} \frac{\vec{f} \cdot \vec{\sigma}}{|\vec{f}|} \quad (2.7)$$

where $f_i = f(x_i)$ and $f(x) = \sin(\pi x)(1 + B \cos^2(\pi x))$, with $B = -0.172$. Notice that $f(x)$ is very similar to $m(x + 1/2)$. Changing the value of B to C does not change significantly the quality of the fit.

Now we turn our interest towards computing $\mathbf{A}_i(\vec{x}, t)$ in the previously mentioned gauge. To extract these quantities from our lattice results implies some lengthy procedure. Apart from the typical order a errors we have to deal with some other sources of errors. Some errors arise through the gauge fixing procedure due to the finite value of N_t/N_s . In this case \mathbf{A}_i is never a pure gauge and cannot be set to zero. Nevertheless these errors are for most purposes quite small and can be monitored by varying N_t/N_s . Our procedure to evaluate the gauge fixing on the lattice configuration is as follows. To evaluate the gauge fixed value of a lattice link $\mathbf{U}_\mu(n)$, we choose a lattice path going through this link and starting and ending at some point P . This point is situated on the surface of minimum energy (smallest time $n_t = -(N_t - 1)/2$) and the path is made of three pieces γ_1 , γ_2 and γ_3 . The first and last paths are situated on the surface of time coordinate $-(N_t - 1)/2$. γ_1 joins P with $P' = (-\frac{(N_t-1)}{2}, \vec{n})$, the point with equal spatial coordinates as the origin of the link $\mathbf{U}_\mu(n)$. γ_3 joins $P'' = (-\frac{(N_t-1)}{2}, \vec{n} + \hat{\mu})$ with P . γ_2 moves from P' along the positive time direction, then goes through the link in question, and then back to P'' along the negative time direction. We complete our gauge fixing by performing a global gauge transformation $\Omega(P)$ which rotates the spatial Polyakov loops Ω_i starting at point P to the values $i\sigma_i$. Summarising these transformations we write down the expressions for the gauge transformed link $\mathbf{U}'_\mu(n)$:

$$\mathbf{U}'_\mu(n) = \Omega(P)\mathbf{U}_{\gamma_1}\mathbf{U}_{\gamma_2}\mathbf{U}_{\gamma_3}\Omega^\dagger(P) \quad (2.8)$$

Indeed, if the spatial links at the smallest time are a pure gauge configuration, \mathbf{U}_{γ_1} and \mathbf{U}_{γ_3} can be gauged to I . And since in the temporal gauge $\mathbf{U}_{\gamma_2} = \mathbf{U}_\mu(n)$, we see that $\mathbf{U}'_\mu(n)$ is really our gauge fixed link.

In addition, the position of P and the choice of γ_1 and γ_3 are irrelevant. However, as mentioned previously we do not exactly have a pure spatial gauge for $-(N_t - 1)/2$ and the actual choice of γ_1 and γ_3 is relevant. To preserve the fact that $\mathbf{U}'_\mu(n)$ (Eq.(2.8)) is a gauge transformed of $\mathbf{U}_\mu(n)$, one must choose P , γ_1 and γ_3 in a predetermined way for all lattice links. Our choice is as follows. The path γ_1 is obtained by running first in the 1 direction, next in the 2 direction and finally in the 3 direction. We finally obtain:

$$\mathbf{U}'_\mu(n) = \Omega(P)\mathbf{L}(n)\mathbf{U}_\mu(n)\mathbf{L}^\dagger(n + \hat{\mu})\Omega^\dagger(P) \quad (2.9)$$

with

$$\begin{aligned} \mathbf{L}(n) = & \prod_{q_1=0}^{n'_1-1} \mathbf{U}_1(P + q_1\hat{e}_1) \cdot \prod_{q_2=0}^{n'_2-1} \mathbf{U}_2(P + n'_1\hat{e}_1 + q_2\hat{e}_2) \cdot \\ & \prod_{q_3=0}^{n'_3-1} \mathbf{U}_3(P + n'_1\hat{e}_1 + n'_2\hat{e}_2 + q_3\hat{e}_3) \cdot \prod_{q_0=0}^{n'_0-1} \mathbf{U}_0(P + n'_1\hat{e}_1 + n'_2\hat{e}_2 + n'_3\hat{e}_3 + q_0\hat{e}_0) \end{aligned} \quad (2.10)$$

where $n'_\mu = n_\mu - P_\mu$ and P_μ are the coordinates of point P .

Once the data are gauge fixed we can extract the lattice approximants to the continuum fields. The potentials A_i^a are taken to lie on the mid-point of the corresponding links. The magnetic fields B_i^a , are computed by the plaquette averages mentioned before. Our results show the same qualitative features for both vector potentials and magnetic fields. These features are described by the following functional form which fits the data:

$$\begin{aligned}
O_1^1 &= q_1(t) \cos(\pi y) \cos(\pi z) (1 + q_2(t)\cos(2\pi x)) \\
&\quad (1 + q_3(t) \cos(2\pi y)) (1 + q_3(t)\cos(2\pi z)) \\
O_1^2 &= (1 + a_1(t) \cos(2\pi x)) (1 + a_2(t)\cos(2\pi z)) \\
&\quad [a_3(t) \sin(\pi z) \cos(\pi x) (1 + a_4(t)\cos(\pi y)) \\
&\quad + a_5(t) \cos(\pi z) \sin(\pi x) \sin(2\pi y)] \\
O_1^3 &= (1 + a_1(t) \cos(2\pi x)) (1 + a_2(t)\cos(2\pi y)) \\
&\quad [-a_3(t) \sin(\pi y) \cos(\pi x) (1 + a_4(t)\cos(\pi z)) \\
&\quad + a_5(t) \cos(\pi y) \sin(\pi x) \sin(2\pi z)]
\end{aligned} \tag{2.11}$$

where O_i^a stands for either B_i^a , E_i^a or A_i^a , but with different values of the parameters q_i and a_i . The remaining components of O_i^a can be obtained by cyclic permutations of the indices 1,2,3 in Eq.(2.11). The values of the parameters appearing in the expression are given in tables 1 to 4.

The previous functional form describes satisfactorily the data with a maximum χ^2 per degree of freedom equal to 4 for A_i^a and 6 for B_i^a . It can be used to study the main features of the solution. Another interesting aspect of the formula is to serve as a guide for the construction of an ansatz which could lead to an analytic expression of the solution. In the following section we will describe the steps that we have taken in this direction.

3 Ansatz

In Eq.(2.11) we have given an analytic expression which describes our numerical results within errors. It is clear that the solution is not as simple as that expression, but we want to explore the consequence of the fact that it shares with it the same behaviour under the symmetry operations of the system. Thus, we will assume the following general form for the solution (for all t):

$$A_i^a = \delta_i^a Q^{(1)}(t, x_i, x_j, x_k) + (\epsilon^{iab})^2 Q^{(2)}(t, x_i, x_a, x_b) + \epsilon^{iab} Q^{(3)}(t, x_i, x_a, x_b) \tag{3.1}$$

where $Q^{(1)}(t, x, y, z) = Q^{(1+)}(t, x, y, z)$ is symmetric under the exchange of y and z , even in all the three variables, antiperiodic in y and z , periodic in x . $Q^{(2)}(t, x, y, z)$ is odd in x, y , even in z , antiperiodic in x, z and periodic in y . $Q^{(3)}(t, x, y, z)$ is odd in the third variable and even in the other two, antiperiodic in x, z and periodic in y . The previous expression implies that the solution is cubic symmetric with $A_i^a(\vec{x})$ and $B_i^a(\vec{x})$ transforming in the $T_1 \otimes T_1$ representation of this group (T_1 is just the spin 1 representation of rotations). In addition, the behaviour under translations by one period is just what is required by the twisted boundary conditions. The previous properties are more restrictive than what can be deduced by these symmetry properties alone. More precisely $Q^{(1)}(t, x, y, z)$ could contain an additional term $Q^{(1-)}(t, x, y, z)$ which is odd in all three variables, antiperiodic

and antisymmetric in the two last variables y, z . To test the presence or absence of this term we have added to A_1^1 in the parametrization Eq.(2.11) a term

$$q_4 \sin(2\pi x) \sin(\pi y) \sin(\pi z) (\cos(2\pi y) - \cos(2\pi z)) \quad (3.2)$$

and refitted our data for \mathbf{A} and \mathbf{B} . The presence of a such a term improves the value of the χ^2 by a factor 2/5, but the size of q_4 and thus its contribution is of the order of the estimated size of the $O(a)$ errors. Thus, we will keep an open attitude and explore both possibilities.

Another additional information which might be crucial for finding the analytic expression is the behaviour under $P \cdot T$. Both parity and time reversal map instantons into anti-instantons, but one could ask whether the product of these two leaves our solution invariant or not. The implications of this invariance are complicated by the future-past asymmetry of our gauge choice. Invariance under $P \cdot T$ implies

$$-\mathbf{A}_i(-\vec{x}, -t) = \mathbf{\Omega}_0^\dagger \mathbf{A}_i(\vec{x}, t) \mathbf{\Omega}_0 + i \mathbf{\Omega}_0^\dagger \partial_i \mathbf{\Omega}_0 \quad (3.3)$$

where $\mathbf{\Omega}_0$ is the gauge matrix which describes the pure gauge at $t = \infty$. The matrix $\mathbf{\Omega}_0$ was parametrised by Eq.(2.7) and indeed the form of the axis of rotation $\vec{f}/|\vec{f}|$ is precisely consistent with the restricted form where $Q^{(1)} = Q^{(1+)}$ even in all three variables. The necessary and sufficient condition for the gauge field at ∞ to be of the restricted form $Q^{(1-)} = 0$ is that f_i is a function of x_i alone.

Expression (3.3) conflicts nevertheless with the requirement $Q^{(1-)} = 0$ since in principle a rotation by $\mathbf{\Omega}_0$ does not preserve this constraint. If we impose that a general rotation around $\vec{f}/|\vec{f}|$ should preserve $Q^{(1-)} = 0$ we must have

$$Q^{(2)}(t, x, y, z) = f(y) \hat{Q}^{(2)}(t, x, y, z) \quad (3.4)$$

$$Q^{(3)}(t, x, y, z) = f(z) \hat{Q}^{(3)}(t, x, y, z) \quad (3.5)$$

where $\hat{Q}^{(2)}(t, x, y, z)$ and $\hat{Q}^{(3)}(t, x, y, z)$ are symmetric functions of the last two arguments y, z . We have verified that these additional constraints are reasonably well satisfied by our data. Thus, we arrive at a restricted parametrization consistent with our data:

$$A_i^a(\vec{x}, t) = \rho_1^i \frac{f_i f_a}{|\vec{f}|} + \rho_2^i |\vec{f}| (\delta_i^a - \frac{f_i f_a}{|\vec{f}|^2}) + \rho_3^i \epsilon_{abi} f_b \quad (3.6)$$

where ρ_1^i , ρ_2^i and ρ_3^i must be even functions of the three variables x, y, z . ρ_1^i and ρ_2^i are periodic in x_i and antiperiodic in $x_j \neq x_i$, and ρ_3^i is antiperiodic in x_i and periodic in $x_j \neq x_i$.

The fact that this form is not a mere consequence of the symmetry properties implies that, when requiring self-duality of such a solution, new equations will arise which guarantee the form to be preserved.

To start with, let us perform a time independent gauge transformation and write

$$\mathbf{A}'_i(\vec{x}, t) = \mathbf{\Omega}_0^{-1/2} \mathbf{A}_i(\vec{x}, t) \mathbf{\Omega}_0^{1/2} + i \mathbf{\Omega}_0^{-1/2} \partial_i \mathbf{\Omega}_0^{1/2} \quad (3.7)$$

This new vector potential complies also to the form Eq.(3.6) in what respects to the behaviour of the ρ' functions under parity. In addition it must satisfy $-\mathbf{A}'_i(-\vec{x}, -t) =$

$\mathbf{A}'_i(\vec{x}, t)$. This implies that $\rho'_1{}^i$ and $\rho'_2{}^i$ are odd in t and $\rho'_3{}^i$ is even in t . We have explicitly checked these properties in our numerical data and found agreement within errors. In fact, given self-duality it is enough that $\rho'_1{}^i = \rho'_2{}^i = 0$ at $t = 0$ to guarantee the appropriate behaviour for $t \neq 0$. At $t = 0$ we have been able to fit both \mathbf{A}_i and \mathbf{B}_i with $\rho'_3{}^i$ alone.

Imposing now self-duality we obtain six equations rather than three. The first set of equations follows from the requirement that the $\rho'_a{}^i$ should have the required behaviour under parity. The equations are:

$$\epsilon^{ijk}(\nabla_j \hat{\rho}'_a{}^k + T^{abc} \hat{\rho}'_b{}^j \hat{\rho}'_c{}^k) = 0 \quad (3.8)$$

where $\nabla_j = \frac{1}{f_j} \partial_j$, $\hat{\rho}'_a{}^i = \rho'_a{}^i + \delta_{a3} \partial_i(f(x_i))/(2|\vec{f}|^2)$ and T^{abc} is a completely antisymmetric tensor with $-T^{123} = T^{231} = T^{312} = 1$.

The solution to this equation is as follows

$$\hat{\rho}'_a{}^i = R^{a\rho\sigma} q_\rho \nabla_i q_\sigma \quad (3.9)$$

where q_ρ satisfy $q_1^2 + q_2^2 - q_3^2 - q_4^2 = 1$ and $R^{a\rho\sigma}$ is a tensor, antisymmetric in the last two indices, with $R^{121} = R^{134} = R^{213} = R^{242} = R^{314} = R^{323} = 1$. The functions q_μ then establish a mapping from $S_1^3 \times \mathfrak{R}$ onto that hyperboloid.

If we now plug the solution for $\hat{\rho}'$ Eq.(3.9) into the self-duality equation, and after considerable massaging, we arrive at

$$\partial_0 s^a = \epsilon^{abc} s_b s'_c \quad (3.10)$$

$$\nabla_i s'_a = \nabla_j \nabla_k s_a \quad (\forall i \neq j \neq k) \quad (3.11)$$

$$s^a s_a = |\vec{f}|^2 \quad (3.12)$$

where indices are raised and lowered with the metric $g_{ab} = \text{diag}(1, -1, -1)$ and $s_1 = |\vec{f}|(q_1^2 + q_2^2 + q_3^2 + q_4^2)$, $s_2 = 2|\vec{f}|(q_2 q_3 - q_1 q_4)$ and $s_3 = 2|\vec{f}|(q_1 q_3 + q_2 q_4)$. The dynamics Eq.(3.10) is consistent with the constraint Eq.(3.12). The most important restriction follows from the integrability condition of Eq.(3.11), which together with Eq.(3.12) serves to restrict the possible value of $f(x)$. If we introduce the function $z_i \equiv z(x_i)$ by the condition $\frac{dz(x)}{dx} = f(x)$, Eq.(3.11) forces s_a to be sum of single variable functions of the variables $a_1 z_1 + a_2 z_2 + a_3 z_3$ with $a_i = +1, -1$ or 0 and $\sum a_i = 1(\text{mod}2)$. On the other hand $|\vec{f}|^2$ is a sum $F(z_1) + F(z_2) + F(z_3)$. One class of solutions is given by functions $s_a(z_1 + z_2 + z_3)$. In this case Eq.(3.12) forces $f(x) = Ax$ and then the whole problem possesses spherical symmetry $z_1 + z_2 + z_3 \propto |\vec{x}|^2$. We are then in the situation discussed in Ref.9 and our equations recover all the axially symmetric solutions including the B.P.S.T.[10] one. It is not easy to find other solutions of Eq.(3.11) and Eq.(3.12). Indeed, if we impose these conditions on the coefficients of the Taylor expansion of the functions $s_a(z)$, the number of conditions grows faster than the number of parameters. This suggests to try polynomials for the functions s_a . In this way we have discovered other solutions, most remarkably one which is defined on the torus with $z = A \cos(Bx + C)$ and where s_1 and s_3 are polynomials of second degree in z_i and s_2 of first degree. The solution goes to a pure gauge in $t \rightarrow \pm\infty$ but is singular at $t = 0$ and the total action is divergent (in the unit cell). We have been unable to find any solution which is satisfactory and coincides with our numerical data.

If our solution does not follow from Eqs.(3.10)-(3.12), one has to drop some of the assumptions leading to those equations. Most likely it is Eq.(3.6) with the assumed properties for ρ_a^i which is wrong, since its validity is simply based on the ability to describe the data. Unfortunately, if we go back to the form Eq.(3.1) with $Q^{(1)} = Q^{(1+)} + Q^{(1-)}$ we have no additional equations which could allow an analytic development of the sort leading to Eqs.(3.10)-(3.12). One can simply rewrite the self duality equations for the Q functions, but we do not know how to select solutions going to a pure gauge in $t = \pm\infty$.

4 Summary and conclusions

In this paper, we have studied the instanton-like solution which occurs in a 3-torus with symmetric twist. It is remarkable that the cooling method provides a very accurate description of this solution which allows a systematic analysis of its properties. Our results imply that there are indeed four instanton and four anti-instanton solutions, all of which are (within errors) cubic symmetric and $P \cdot T$ invariant. The solution is also smooth, although singularities in sufficiently high derivatives are not excluded. We have given functional forms which incorporate the previously mentioned properties, plus additional restrictions consistent with the data. Nonetheless, the more restrictive form, which allows the reduction of the problem to motion on a hyperboloid and recovers many multi-instanton solutions on S_4 does not seem to contain the solution of our problem.

Acknowledgements

This work has been partially financed by CICYT.

Table Captions

Table 1: The value of the parameters obtained when fitting the functional form (2.11) and (3.2) to the $N_s = 11$, $N_t = 29$ data for A_1^1 . $n_t = 15$ corresponds to the time of maximum energy. Errors are indicated by giving within parenthesis their magnitude affecting the last quoted digit.

Table 2: The same as Table 1 but for the parameters entering in A_1^2 , A_1^3 .

Table 3: The same as Table 1 but for the data of B_1^1 .

Table 4: The same as Table 2 but for the data of B_1^2 , B_1^3 .

Figure Captions

Fig.1: The scalar product $M_{12} = \vec{E}_1 \cdot \vec{E}_2$ plotted as a function of x for $y = 0.209$ and $z = 0$. The squares correspond to the lattice values for $N_s = 11$, $N_t = 21$. They are compared to the prediction of Eq.(2.3).

Fig.2: $m_0(t)$ appearing in Eq(2.5) is plotted as a function of time for $N_s = 11$, $N_t = 21$. The continuous line represents the function $\cos(\frac{\pi}{2}\tanh(0.69\pi t))$.

Table 1

nt	q₁	q₂	q₃	q₄
5	0.094(8)	0.04(6)	0.02(6)	0.00(1)
6	0.140(8)	0.05(2)	0.02(2)	0.00(1)
7	0.208(8)	0.06(3)	0.02(3)	0.00(1)
8	0.302(8)	0.07(2)	0.02(2)	0.00(1)
9	0.438(8)	0.09(1)	0.03(2)	0.00(1)
10	0.624(8)	0.103(9)	0.043(9)	0.00(1)
11	0.870(8)	0.120(6)	0.058(7)	0.01(1)
12	1.182(6)	0.138(4)	0.078(5)	0.02(1)
13	1.550(6)	0.154(3)	0.102(4)	0.02(1)
14	1.954(6)	0.167(3)	0.129(3)	0.03(1)
15	2.356(6)	0.177(1)	0.156(2)	0.05(1)
16	2.716(6)	0.182(2)	0.182(2)	0.07(1)
17	3.010(6)	0.184(1)	0.205(2)	0.09(1)
18	3.234(6)	0.183(1)	0.224(2)	0.11(1)
19	3.392(6)	0.181(1)	0.240(2)	0.12(1)
20	3.498(6)	0.179(1)	0.252(2)	0.13(1)
21	3.566(6)	0.178(1)	0.261(2)	0.14(1)
22	3.610(6)	0.176(1)	0.267(2)	0.14(1)
23	3.638(6)	0.175(1)	0.272(2)	0.14(1)
24	3.654(6)	0.174(1)	0.276(2)	0.14(1)
25	3.664(6)	0.174(1)	0.278(2)	0.14(1)
26	3.672(6)	0.173(1)	0.280(2)	0.14(1)
27	3.674(6)	0.173(1)	0.282(2)	0.14(1)
29	3.674(6)	0.172(1)	0.284(2)	0.14(1)

Table 2

nt	a_1	a_2	a_3	a_4	a_5
6	0.00(6)	-0.02(6)	-0.122(6)	0.07(4)	-0.002(6)
7	0.01(5)	-0.03(4)	-0.172(6)	0.09(3)	0.008(6)
8	0.01(3)	0.01(3)	-0.244(6)	0.11(2)	0.018(6)
9	0.01(2)	0.03(2)	-0.348(6)	0.14(2)	0.034(6)
10	0.02(1)	0.04(1)	-0.496(6)	0.15(1)	0.062(6)
11	0.02(8)	0.07(1)	-0.704(6)	0.19(8)	0.109(6)
12	0.033(6)	0.092(5)	-0.984(6)	0.225(6)	0.174(6)
13	0.042(5)	0.118(5)	-1.344(6)	0.253(4)	0.272(6)
14	0.052(4)	0.145(4)	-1.776(6)	0.278(3)	0.402(6)
15	0.060(3)	0.169(3)	-2.258(6)	0.298(3)	0.558(6)
16	0.065(3)	0.189(2)	-2.746(6)	0.311(2)	0.730(6)
17	0.068(2)	0.204(2)	-3.200(6)	0.314(2)	0.902(6)
18	0.069(2)	0.215(2)	-3.590(6)	0.324(2)	1.056(6)
19	0.069(2)	0.221(2)	-3.902(6)	0.325(2)	1.186(6)
20	0.067(2)	0.225(1)	-4.138(6)	0.325(1)	1.290(6)
21	0.065(2)	0.227(2)	-4.312(6)	0.324(1)	1.368(6)
22	0.064(2)	0.229(1)	-4.434(6)	0.323(1)	1.424(6)
23	0.063(2)	0.230(1)	-4.520(6)	0.322(1)	1.436(6)
24	0.062(2)	0.230(1)	-4.580(6)	0.321(1)	1.494(6)
25	0.061(2)	0.231(1)	-4.620(6)	0.320(1)	1.514(6)
26	0.061(2)	0.231(1)	-4.648(6)	0.320(1)	1.530(6)
27	0.061(2)	0.231(1)	-4.666(6)	0.320(1)	1.540(6)
29	0.061(2)	0.232(1)	-4.686(6)	0.320(1)	1.554(6)

Table 3

nt	q ₁	q ₂	q ₃	q ₄
3	0.216(8)	0.04(3)	0.00(3)	0.00(1)
5	0.424(8)	0.06(1)	0.01(2)	0.00(1)
6	0.610(8)	0.07(8)	0.02(1)	0.00(1)
7	0.876(8)	0.090(5)	0.026(8)	0.00(1)
8	1.246(8)	0.109(4)	0.038(6)	0.01(1)
9	1.736(8)	0.130(3)	0.054(4)	0.01(1)
10	2.352(8)	0.152(2)	0.077(3)	0.03(1)
11	3.058(8)	0.175(2)	0.107(2)	0.05(1)
12	3.760(8)	0.196(1)	0.144(2)	0.08(1)
13	4.300(8)	0.213(1)	0.191(2)	0.12(1)
14	4.504(8)	0.223(1)	0.244(2)	0.17(1)
15	4.278(6)	0.224(1)	0.301(2)	0.21(1)
16	3.682(8)	0.216(1)	0.361(2)	0.23(1)
17	2.900(8)	0.200(2)	0.421(2)	0.21(1)
18	2.124(8)	0.181(2)	0.482(3)	0.17(1)
19	1.474(6)	0.160(3)	0.542(5)	0.12(1)
20	0.986(6)	0.141(4)	0.603(7)	0.08(1)
21	0.644(6)	0.124(6)	0.663(1)	0.04(1)
22	0.412(6)	0.108(8)	0.73(1)	0.03(1)
23	0.264(6)	0.09(1)	0.79(3)	0.01(1)
24	0.166(6)	0.08(2)	0.87(4)	0.00(1)
26	0.062(6)	0.03(4)	1.1(1)	0.00(1)

Table 4

nt	a₁	a₂	a₃	a₄	a₅
3	0.00(6)	0.00(6)	-0.120(6)	0.07(4)	0.006(6)
5	0.01(2)	0.02(3)	-0.292(6)	0.10(2)	0.022(6)
6	0.01(2)	0.02(2)	-0.438(6)	0.12(1)	0.042(6)
7	0.02(1)	0.04(1)	-0.644(4)	0.147(8)	0.074(6)
8	0.019(2)	0.050(8)	-0.940(6)	0.177(6)	0.132(6)
9	0.027(5)	0.069(5)	-1.354(6)	0.210(4)	0.224(6)
10	0.037(4)	0.095(4)	-1.912(3)	0.245(3)	0.370(6)
11	0.050(3)	0.126(3)	-2.626(6)	0.280(2)	0.584(6)
12	0.064(2)	0.161(2)	-3.464(6)	0.313(2)	0.872(6)
13	0.079(2)	0.198(1)	-4.322(6)	0.341(1)	1.212(6)
14	0.092(2)	0.233(1)	-5.018(6)	0.361(1)	1.550(6)
15	0.100(2)	0.262(1)	-5.354(6)	0.372(1)	1.796(6)
16	0.100(2)	0.282(1)	-5.214(6)	0.372(1)	1.880(6)
17	0.093(2)	0.293(1)	-4.754(6)	0.364(1)	1.786(6)
18	0.080(2)	0.297(2)	-3.950(6)	0.349(2)	1.556(6)
19	0.064(3)	0.294(2)	-2.998(6)	0.331(2)	1.264(6)
20	0.047(4)	0.289(3)	-2.232(6)	0.312(3)	0.974(6)
21	0.031(5)	0.282(4)	-1.608(6)	0.293(4)	0.724(6)
22	0.017(7)	0.276(6)	-1.132(6)	0.277(3)	0.522(6)
23	0.00(1)	0.271(8)	-0.784(6)	0.264(8)	0.370(6)
24	0.00(1)	0.27(1)	-0.536(3)	0.26(1)	0.230(6)
25	0.00(2)	0.28(1)	-0.364(6)	0.26(2)	0.180(6)
26	0.00(3)	0.30(2)	-0.244(6)	0.27(3)	0.130(6)
29	0.00(3)	0.30(2)	-0.244(6)	0.27(3)	0.130(6)

References

- [1] G. 't Hooft, Nucl. Phys. 153 (1979) 141.
G. 't Hooft, Acta Phys. Austriaca Suppl. 22 (1980) 531.
- [2] A. González-Arroyo, C.P. Korthals Altes, Nuc. Phys. B311 (1988/89) 433.
- [3] S. Sedlacek, Comm. Math. Phys. 86 (1982) 515.
- [4] M. García Pérez, A. González-Arroyo, B. Söderberg, Phys.Lett. B235 (1990) 117.
- [5] B. Berg, Phys. Lett. B104 (1981) 61;
M. Teper, Phys. Lett. B162 (1985) 357.
- [6] G. 't Hooft, Comm. Math. Phys. 81 (1981) 267.
P. van Baal, Twisted boundary conditions: a non perturbative probe for pure non-abelian gauge theories, Ph.D. Thesis, Utrecht (1984).
- [7] P. van Baal and N.D. Hari Dass, THU-92/03, ITFA-92/01 Utrecht preprint, January 1992.
- [8] T. Hansson, P. van Baal and I. Zahed, Nucl. Phys. B289 (1987) 682.
D. Daniel, A. González-Arroyo, C.P. Korthals Altes and B. Söderberg, Phys. Lett. B221 (1989) 136.
- [9] E. Witten, Phys. Rev. Lett. 38 (1977) 121.
- [10] A. Belavin et al, Phys. Lett. B59 (1975) 85.

Fig.1

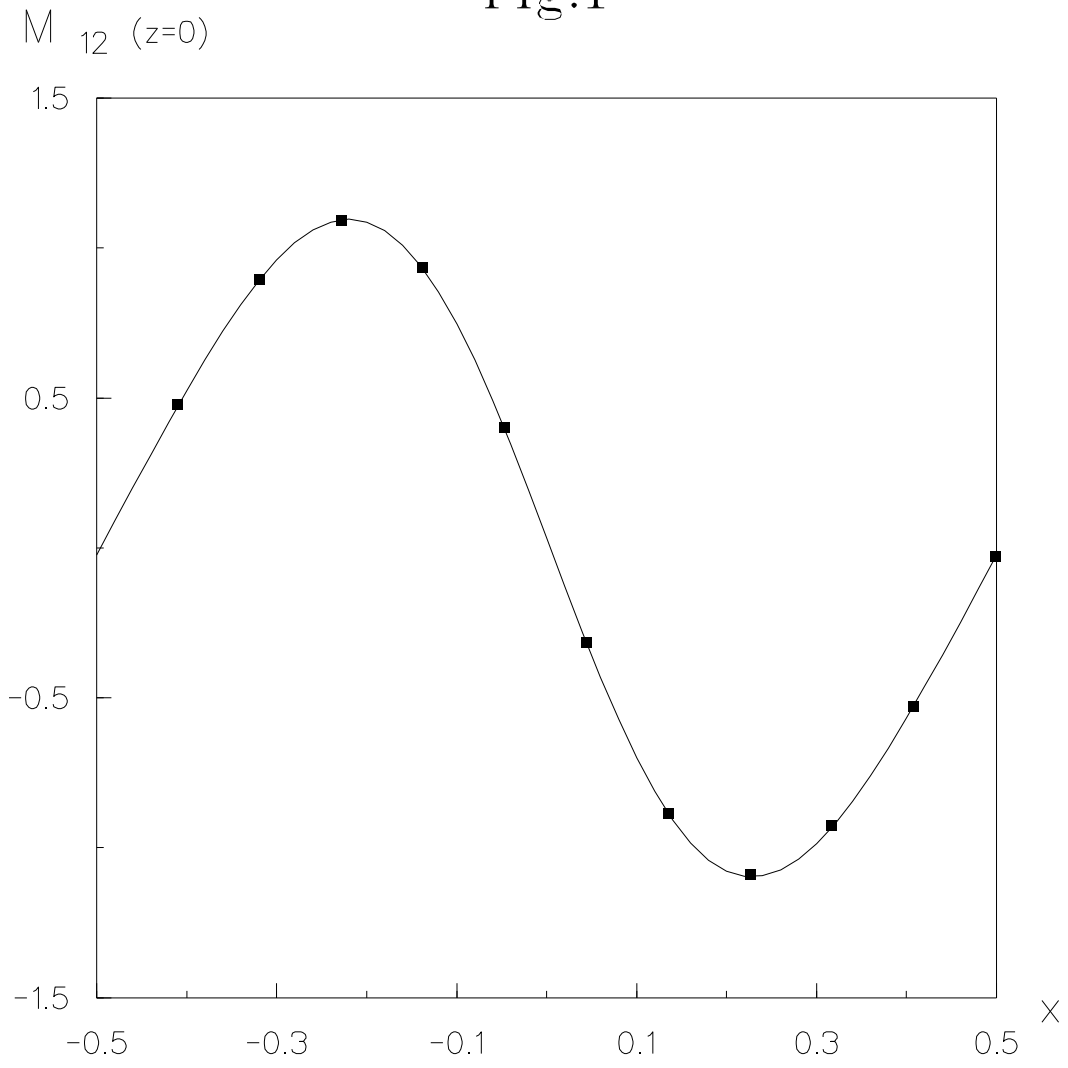


Fig.2

